CDK9 a Potential Target for Drug Development

Fernanda Canduri[1], Patrícia Cardoso Peres[2], Rafael Andrade Caceres[2] and Walter Filgueira de Azevedo Jr.[2,*]

[1]*Departamento de Química e Física Molecular, Instituto de Química de São Carlos, Universidade de São Paulo, Av. Trabalhador Sãocarlense, 400. São Carlos-SP, Brazil;* [2]*Faculdade de Biociências-PUCRS-Av. Ipiranga,6681. Porto Alegre-RS Brazil*

Abstract: The family of Cyclin-Dependent Kinases (CDKs) can be subdivided into two major functional groups based on their roles in cell cycle and/or transcriptional control. CDK9 is the catalytic subunit of positive transcription elongation factor b (P-TEFb). CDK9 is the kinase of the TAK complex (Tat-associated kinase complex), and binds to Tat protein of HIV, suggesting a possible role for CDK9 in AIDS progression. CDK9 complexed with its regulatory partner cyclin T1, serves as a cellular mediator of the transactivation function of the HIV Tat protein. P-TEFb is responsible for the phosphorylation of the carboxyl-terminal domain of RNA Pol II, resulting in stimulation of transcription. Furthermore, the complexes containing CDK9 induce the differentiation in distinct tissue. The CDK9/cyclin T1 complex is expressed at higher level in more differentiated primary neuroectodermal and neuroblastoma tumors, showing a correlation between the kinase expression and tumor differentiation grade. This may have clinical and therapeutical implications for these tumor types. Among the CDK inhibitors two have shown to be effective against CDK9: Roscovitine and Flavopiridol. These two inhibitors prevented the replication of human immunodeficiency virus (HIV) type 1 by blocking Tat transactivation of the HIV type 1 promoter. These compounds inhibit CDKs by binding to the catalytic domain in place of ATP, preventing transfer of a phosphate group to the substrate. More sensitive therapeutic agents of CDK9 can be designed, and structural studies can add information in the understanding of this kinase. The major features related to CDK9 inhibition will be reviewed in this article.

Key Words: CDK9, drug-design, molecular modeling.

INTRODUCTION

Cell cycle progression is controlled by cyclin-dependent kinases (CDKs) [1-3]. CDKs (EC 2.7.11.22) are part of a family of serine/threonine protein kinases that play a key role in the regulation of progression through the cell division cycle. In each phase of the cell cycle CDKs phosphorylate distinct proteins and therefore are usually classified as either G1 (CDK4 and CDK6/cyclins D, CDK2/cyclin E), S (CDK2/cyclin A, CDK1/cyclin A), or G2/M (CDK1/cyclin B) phase specific [4,5]. Human CDKs are inactive as monomers and regulation of these kinases is tightly controlled at different levels, including interactions with negative and positive partners, activation by de/phosphorylation and subcellular localization.

Besides the role in cell cycle regulation, several CDKs participate in other physiological processes, such as neuronal function (CDK5, CDK11), apoptosis (CDK1, CDK5) and transcription (CDK2, CDK7, CDK8, CDK9, CDK11), which are also affected by pharmacological inhibitors of CDKs [6,7][9, 23]. Especially the latter one has recently attracted medicinal chemists, because roles of CDKs in many viral infections have been established. Small DNA viruses rely on host cell CDK2 for their replication, some require host expression apparatus (CDK2-activated) to synthesize replication proteins, while others encode their own cyclins that activate cellular CDKs, or contain proteins that directly recruits CDKs to the nascent viral transcripts to finish its synthesis [8].

Since deregulation of cyclins and/or alteration or absence of CDK inhibitors (CKIs) has been associated with many cancers, there is strong interest in chemical inhibitors of CDKs that could play an important role in the discovery of new family of antitumor agents [9]. Therefore, namely CDK2 and 4 became very often investigated as promising protein targets for development of novel anticancer agents [10-13]. In addition to the positive regulatory role of cyclins and CDK7, many negative regulatory proteins (CKIs) have been discovered [13]. CKIs fall into two broad categories based upon whether they bind solely to the catalytic subunit (CDK) or whether they bind to CDK complexes. The former category has been identified only in higher eukaryotic cells and is termed the INK family. The most studied INKs are the proteins p15, p16, p18, and p19. These inhibitory proteins bind to CDK4 and 6 and prevent binding of the cyclin partner [14]. Inhibitors of the second category bind to CDK complexes. In mammalian cells, this family includes protein p21, p27, and p57 [14]. Besides positive and negative regulation by phosphorylation and binding of cyclins and CKIs, CDKs interact with another class of regulatory proteins known as CskHs. This protein is also known as p9. It was identified two homologues in humans (CskHs1 and CskHs2) [13]. Despite many studies investigating its role in the cell cycle, the function of p9 is not yet understood. The structure of the complex CDK2-p9 has been determined and based on this structure it was proposed that p9 acts in targeting the

*Address correspondence to this author at the Faculdade de Biociências-PUCRS-Av. Ipiranga,6681. Porto Alegre-RS Brazil;
E-mail: walter.junior@pucrs.br

1573-4064/08 $55.00+.00

CDKs to other proteins or macromolecular assemblies [15]. It is clear that phosphorylation of serine, threonine and tyrosine residues is of major importance in all aspects of cell life and protein kinases are pharmacological targets [6].

ATP is the authentic cofactor of CDK it can be considered as a "lead compound" for discovery of CDK inhibitors. However, there are two major concerns: adenine containing compounds are common ligands for many enzymes in cells, thus, and adenine derivatives may inhibit other enzymes in the cells; second, any highly charged groups such as phosphates in ATP will prevent uptake by cells [16].

Over 80 CDK2 inhibitors have now been described, some of then presents IC50 at nanomolar concentrations [17]. During the past decade many potent and selective inhibitors of CDKs were developed in the SAR drug discovery programs, in spite of a relevant degree of active site similarity across the realm of protein kinases. The structures of binary complexes between CDK2 with several different inhibitors have been described using biocristallography and structural bioinformatics. Recently Canduri & Azevedo [18], proposed a major classification for CDK inhibitors. In this classification the chemical inhibitors of CDK2 are divided in two broad classes considering their specificities. Class I CDK inhibitors are those that are selective for CDK2 (and also CDK1, 5), such as olomoucine, roscovitine, purvalanol B, aminopurvalanol, hymenialdisine, indirubin-3'-monoxime, indirubin-5-sulfonate, SU9516 and alsterpaullone. Class II CDK inhibitors are those that are not selective for any specific CDK, such as deschloroflavopiridol and flavopiridol. Class II inhibitors are not specific for CDK2, although some of them present IC50 in nanomolar concentrations, such as flavopiridol. The effects of CDK inhibitors on the cell cycle progression and their potential value for the treatment of cancer have been extensively studied [6,19]. There are three main features that make CDK inhibitors potential anti-tumor agents: 1) They arrest cells in G1 or G2/M. 2) They trigger apoptosis, alone or in combination with other treatments. 3) In some case, inhibition of CDKs contributes to cell differentiation [20-23].

Most of the CDK inhibitors comprise of structurally distinct flat heterocyclic molecules, entering the active site and competing with ATP, a feature usually demonstrated by enzyme kinetics and CDK2-inhibitor co-crystals and CDK9-inhibitor homology models. Anti-CDK drugs possess inhibitory properties against cancer cells both *in vitro* and *in vivo* and some of them (e.g. trisubstituted purine roscovitine, chloroindolyl sulphonamide E7070 and 2-aminothiazole BMS-387032) are hence already evaluated in clinical trials as a new generation of anticancer chemotherapeutics [24]. Efficiency of several CDK inhibitors such as olomoucine, roscovitine and flavopiridol has been demonstrated on life cycles of several viruses and their activity attributed to inhibition of transcription [23-26]. However, also oncology offers a new application for these inhibitors. Despite both *in vitro* and *in vivo* efficiency of CDK2 inhibitors, a rationale for their anticancer application has been displaced by evidence that CDK2 knock-out mice are fully viable [27]. What is the proper reason for activity of these inhibitors is still not clear, but there are strong evidences that more CDKs must be targeted at the same time [17]. In particular, inhibition of CDKs mediating phosphorylation of the C-terminal domain (CTD) of RNA polymerase II is thought to markedly contribute to cytotoxic potency of such compounds, as shown with flavopiridol and roscovitine [28-31]. Pharmacological inhibition of transcription, resulting in rapid decline of the protein levels (especially those where both mRNA and protein have short half-lives), might be the explanation for induction of cell death. One such gene product is the antiapoptotic factor Mcl-1crucial for the survival of a range of cell types, and its down-regulation either by roscovitine or siRNA is sufficient to induce apoptosis [32, 33]. More particularly, selective CDK9 inhibition could also serve as a potential therapeutic strategy against tumor invasion and metastasis, as has been recently demonstrated that inflammatory cytokine tumour necrosis factor-alpha promotes tumour progression through activation of matrix metalloproteinase [17, 34].

Recent progress on the development and analysis of CDK inhibitors already identified several structurally diverse compounds having the ability to block the CDKs' phosphorylating activity [17,35,36]. Newly identified, 4-phenylazo-3,5-diamino-pyrazole inhibitors were found to weakly inhibit the activity of CDK2/cyclin E [17]. Due to the relatively easy synthesis of its derivatives several new protein kinase inhibitors were developed based on this moiety. A total of thirty five 3,5-diaminopyrazole derivatives substituted with different arylazo side chains at position 4 were synthesized to illustrate their structure-activity relationships, and determine their *in vitro* antiproliferative properties on cancer cell lines [17]. This review is focused on the structural basis for specificity of human CDK9 by several different moieties such as flavone derivatives, purines and diaminopyrazole derivatives.

HUMAN CDKs

There are over a hundred close-related serine/threonine protein kinases identified in the human genome, however many of them are result of alternative splicing or present larger sequence, when compared with CDK1 and CDK2, which makes alignment clumsy. Fig. (**1**) shows the sequence alignment of 10 human CDKs. In this alignment we can easily visualize the proximity of CDKs. Analysis of the alignment human CDKs indicates the similarity of CDK9 with CDK8 and CDK7. The sequence dendrogram shown in Fig. (**2**), suggested that the CDK alignment joins the sequences in three sub-families, besides the CDK9 sub-family, there is one sub-family joining CDK1, 2, 3 and 5, and a third cluster joining CDK4, 6 and 10. This information has been successfully used to model CDK1 [37], CDK9 [38], and CDK5 [39], generating reasonable models. These models have been used to establish the structural basis for inhibition of these CDKs.

CLONING, EXPRESSION AND PURIFICATION OF CDK9

In order to perform structural studies, human CDK9 has been produced using pET vector system and *E. coli* BL21 (DE)pLys. The expression in different temperatures was used to yield soluble CDK9. The best condition was obtained by culturing the selected colonies with the plasmid

pET23a(+)::cdk9 in LB medium at 30 °C and 0.1mM IPTG. The expression at 37 °C resulted in high amounts of precipitated proteins; at lower temperature (28 and 20 °C), the expression resulted in low amounts of protein. In respect to IPTG, we found that cultures with lower IPTG concentrations produced appropriate amounts of soluble protein. Almost 40mg.mL^{-1} of total protein was synthesized and the soluble proteins were recovered after centrifugation [40]. The CDK9 obtained following this procedure was used for CD studies, which corroborates the molecular model previously obtained for CDK9 [17].

Circular dichroism is an important technique to estimate secondary structure content, to validate protein homology modeling, and for monitoring conformational changes of proteins due to drug binding. This technique has been employed to assess the CDK9 structure in solution. Analysis of the CD spectrum showed that it contains 30–34% helix, 33–36% beta, and 21–29% of coil. Such CD data permitted to obtain information about the CDK9 structures of the regions not modeled [40]. The results suggest that human recombinant CDK9 maintains secondary structures and is viable to functional and structural studies.

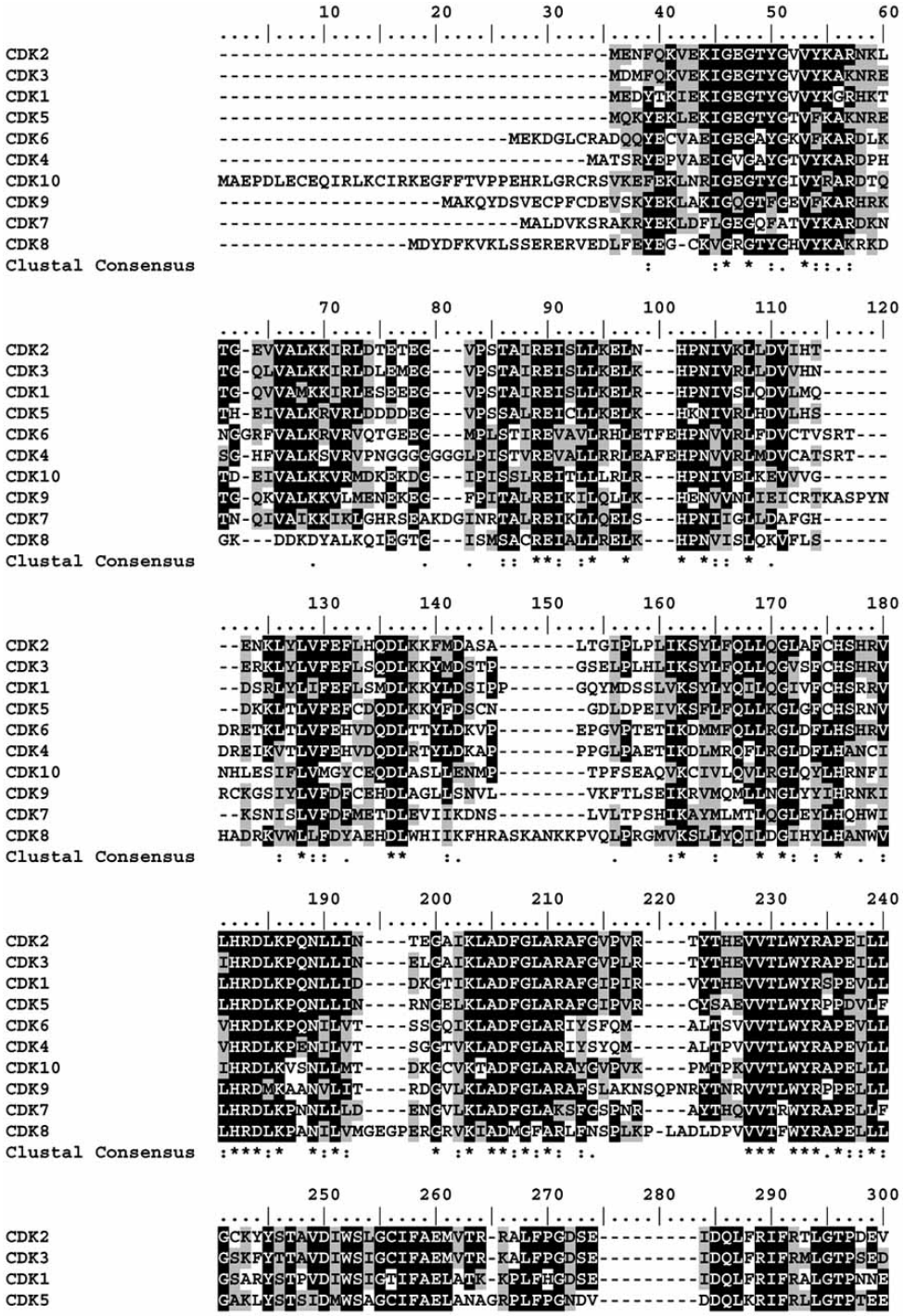

(Fig. 1. Contd….)

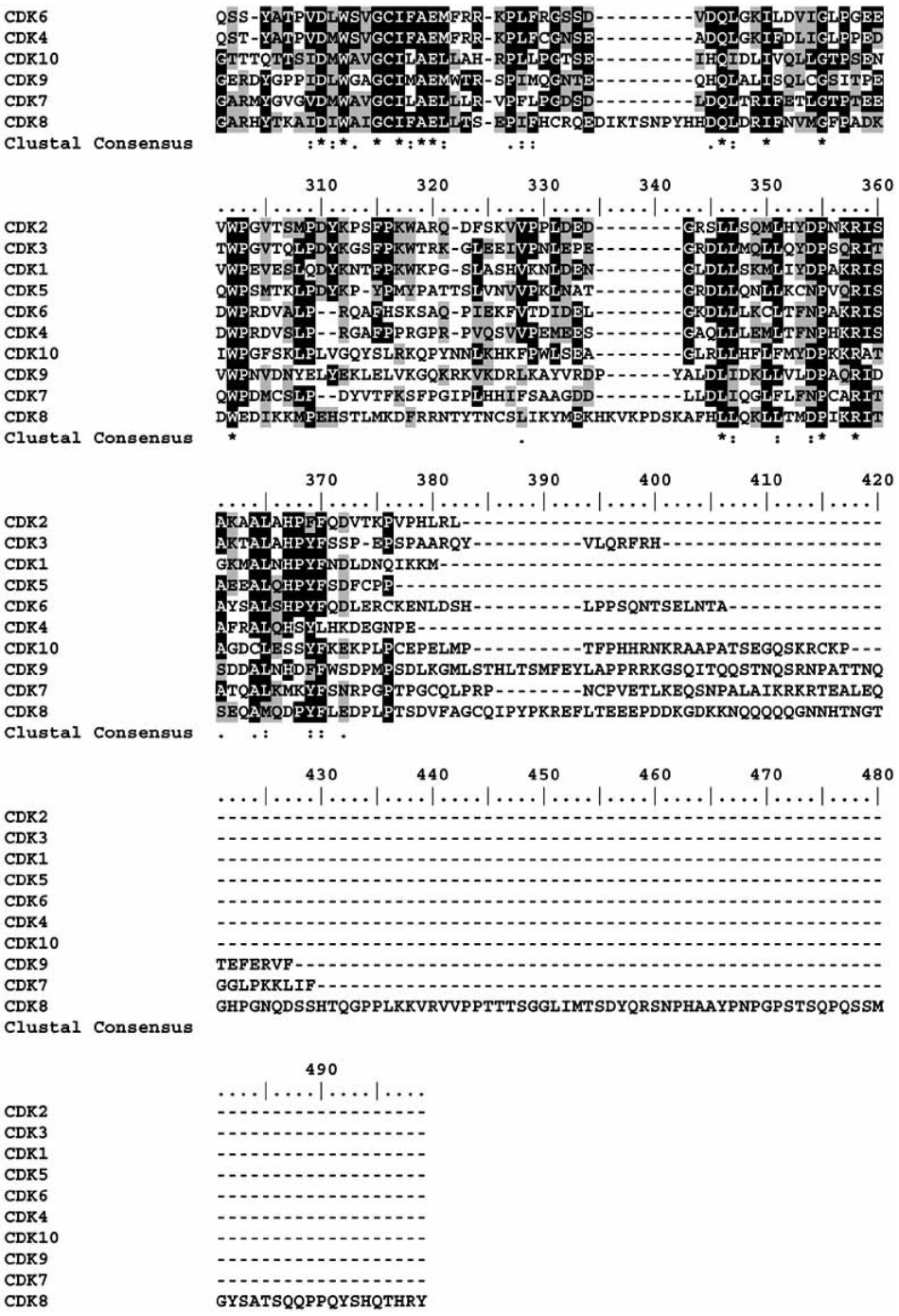

Fig. (1). Sequence alignment of 10 human CDKs generated using BioEdit [58]. The alignment was performed using ClustalW [54].

CDK9 BIOLOGICAL FUNCTIONS

Global Transcriptional Elongation Factor

Transcription by RNA polymerase II (pol II) is a multistep process including preinitiation, initiation, promoter clearance, elongation, and termination [41].

P-TEFb, a positive transcription elongation factor stimulates transcription elongation by phosphorylating Ser2 of the 52 repeats of heptapeptide Tyr-Ser-Pro-Thr-Ser-Pro-Ser of the carboxyl terminal domain (CTD) of the RNA pol II [42], preventing its arrest. P-TEFb is a heterodimeric complex comprised of cyclin-dependent kinase 9 (CDK9) and a regulatory cyclin subunit of the T (T1, T2a, T2b or K1).

Tak and CDK9

Human immunodeficiency virus type 1 (HIV-1) encodes for a protein, Tat, which dramatically activates viral transcription. This simulation occurs through the interaction of

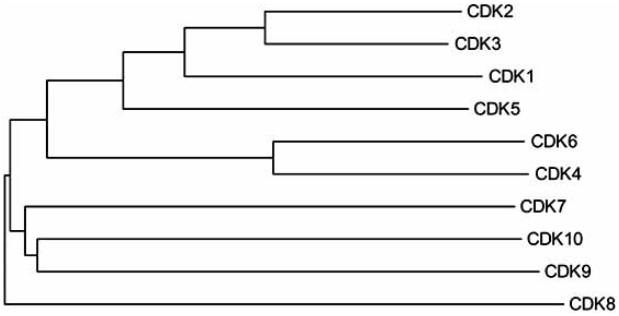

Fig. (2). Sequence dendrogram of the alignment obtained for 10 human CDKs. The alignment was performed using ClustalW [54].

the protein with the transactivator response (TAR) RNA element located at the 5′ end of nascent retroviral transcripts. A Tat-associated kinase (TAK) was isolated, with the ability to phosphorylate CTD. It was identified that CDK9 is the kinase of the TAK complex, showing that TAK is analogous to the P-TEFb [43]. In absence of Tat, phosphorylation of CTD occurs on Ser 2 ad Ser 5; Cdk9 phosphorylates Ser 2, while Cdk7 phosphorylates Ser 5. In presence of Tat, on the other hand, the substrate specificity of Cdk9 is altered, and this kinase phosphorylates both the Ser residues. This suggests that the ability of Tat to increase transcription elongation may be due to its ability to modify the substrate specificity of the Cdk9 complex [44].

CDK9 model

The sequence of Cell division protein kinase 9 (EC 2.7.11.22) (EC 2.7.11.23) (CDK9) consists 372 amino acids with a molecular weight of 42,778 Da and a theoretical pI of 8.97. There is no crystallographic structure available for human CDK9, however the similarity between CDK9 and CDK2 sequence makes CDK2 structure a reasonable template for modelling of CDK9. Azevedo *et al.* using the atomic coordinates of CDK2 generated a homology model for human CDK9, that has also been used to study the structural basis for interaction between CDK9 and inhibitors [38]. To model CDK9 structure it was used Parmodel, a free webserver dedicated to molecular modeling [45]. The alignment of CDK2 (template) and CDK9 (target) is shown in Fig. (**1**). Fifteen residues from the N-terminal and 45 residues from the C-terminus were removed from the CDK9 model, since there is no good template for these fragments. Analysis of the CDK9 structure shows that it belongs to the class of alpha+beta structures and investigation of the fold indicates two alpha+beta domains with a larger C-terminal mostly alpha helical, which is characteristic of the protein-kinase fold. Fig. (**3**) shows the structure of human CDK9 in complex with ATP. As expected the structural model of CDK9 shows a bilobal structure, with smaller N-terminal domain consisting of a sheet of five antiparallel β-strands and a single large α-helix. The larger C-terminal domain consists primarily of α-helices. It contains a pseudo-4-helical bundle, a small β-ribbon and two additional α-helices. The ATP-binding pocket is found in the cleft between the two lobes. The adenine base is positioned in a hydrophobic pocket between the β-sheet of the small domain. In the binary complex of CDK9-ATP the ATP phosphates are held in position by ionic and hydrogen-bonding interactions with several residues, including Lys33, Asp145, and the backbone amides of the glycine-rich loop (residues 10-17). It was observed that ATP binding to CDK9 appears to induce a slight closure of the cleft by a 2^{o} hinge movement around an axis parallel to the longitudinal axis of the ATP molecule, as observed for the crystallographic structure of CDK2 [38]. All inhibitors and ATP bind in the deep cleft between the two domains. Sequence alignment of 10 close related human CDKs (Fig. (**1**)) indicates that these CDKs share several conserved structures, such as: Glycine loop, T loop, and P loop. Fig. (**4**) shows the intermolecular contact between CDK9 and ATP.

Fig. (3). Structure of human CDK9 in complex with ATP solved by molecular modeling [55]. Figure generated using Pymol [56], the protein is presented as ribbon diagram (light gray) and ligand ATP is presented as stick model (dark gray).

Inhibition of CDK9

Based on the structural models obtained for the complexes between CDK9 and different ligands we may highlight few structural features identified on these models that are important for inhibition of CDK9. There is structural information available for CDK9 in complex with flavopiridol [38] and with CAN508 [17], both inhibitors present low molecular weight, below 600 Da, and they are all flat and hydrophobic heterocycles. Fig. (**5**) shows the structural formula for flavopiridol and CAN508. Furthermore, all CDK inhibitors studied so far act by competing with ATP for binding in the CDK ATP-binding pocket [18]. Fig. (**6**) shows the interaction of these two inhibitors with ATP-binding pocket. Most of the contacts are hydrophobic and the complexes present few intermolecular interactions. The inhibitors are enclosed in a hydrophobic pocket formed by Ile10, Ala31, Val64, and Leu134. This hydrophobic environment is conserved in all human CDKs, with one exception at position 31, which is replaced for Asp in the CDK8 sequence. We used the numbering scheme shown for CDK2. Analysis of the contact area between inhibitor and CDK9 indicates that inhibitors with low IC50 values (higher affinity for CDK9) present higher contact areas and higher number intermolecular hydrogen bonds. One of the most studied CDK inhibitor is flavopiridol, which is also one of the most potent inhibitors of HIV-1 transcription and virus replication identified to date.

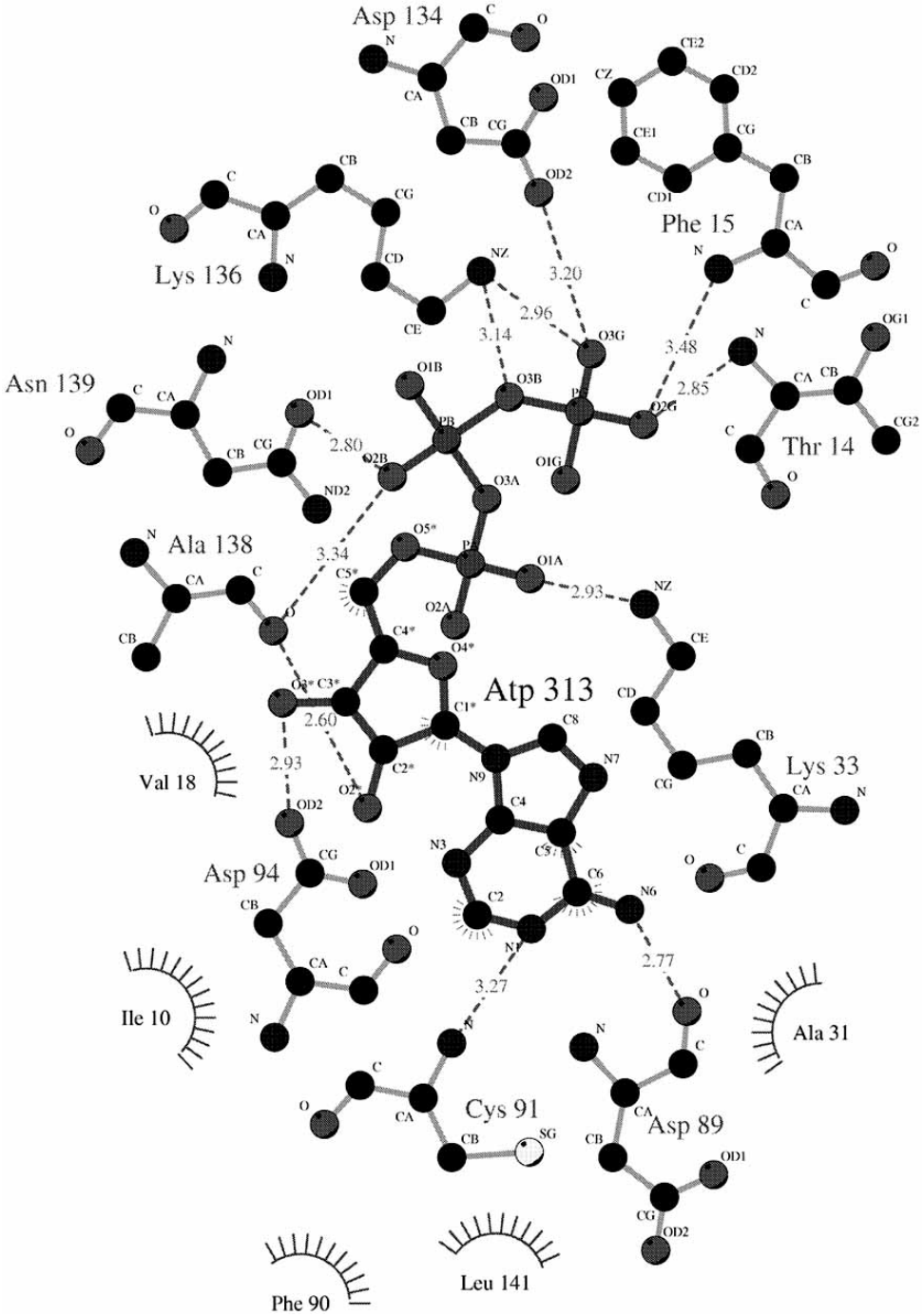

Fig. (4). Intermolecular contacts between CDK9 and ATP. Figure generated with Ligplot [57], the dashed lines shows the hydrogen bonds among CDK9 residues and ATP ligand and its length.

A primary target of flavopiridol is the positive transcription elongation factors b (P-TEFb) kinase. A close inspection of the CDK9 model did not reveal the presence of any additional binding pockets. Furthermore, attempt to dock CDK inhibitors with CDK9 identified the same ATP pocket as a binding site [38]. CDK9-flavopiridol model clearly reveals a very tight binding of the inhibitor to the enzyme, which may essentially inactivate the enzyme, in such scenery a competitive kinetic mechanism is possible.

Analysis of the binary complexes of CDK2 and CDK9 with flavopiridol indicates that the contact areas for the complexes of CDK2 and CDK9 with flavopiridol are 320 $Å^2$ and 332 $Å^2$ respectively, which may partially explain the lower IC50 value observed for CDK9. In addition, the CDK9–flavopiridol complex shows a higher number of intermolecular hydrogen bonds, which also indicates that flavopiridol has higher affinity for CDK9. The structure of the binary complex indicates that the flavopiridol is tightly bound to the ATP-binding pocket and since no further binding sites were

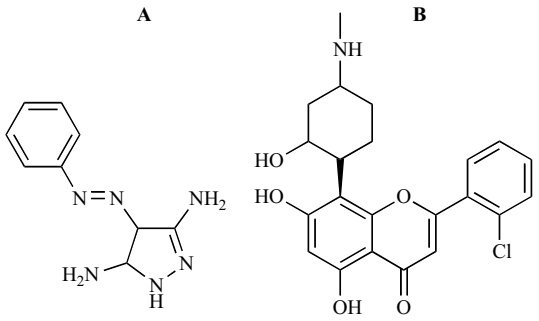

Fig. (5). Structural formula for CAN508 (4-Arylazo-3,5-diamino-pyrazole) (A) and flavopiridol (B).

identified in the CDK9 structure we have strong structural evidence that flavopiridol is a competitive inhibitor with ATP, as observed for the CDK2. Superposition of the complexes of flavopiridol with CDK2 and CDK9 is shown on Fig. (**7**). The benzopyran ring of flavopiridol occupies approximately the same region in both complexes. This region is the same occupied by the purine ring of ATP in the CDK2-ATP complex [16]. Superposition of the CDK2-ATP onto CDK9-flavopiridol structure indicates that the two ring systems overlap approximately in the same plane, but the benzopyran is rotated about 52.5° relative to the adenine in ATP, measured as the angle between the carbon–carbon bonds joining the two cycles in benzopyran and adenine rings, respectively. Two strong salt bridges are observed between Glu 92–Lys 20 and Glu 92–Lys 29 in the CDK9–flavopiridol structure, these salt bridges involve residues from two different lobes of the CDK9 structure and they are not conserved on the CDK2 structure, Lys 20 and 29 in the N-terminal lobe and Glu 92 in the C-terminal lobe. This strong electrostatic interaction brings the two lobes of CDK9 closer, which increases the contact area between enzyme and inhibitor. Fig. (**8**) shows the position of the salt bridges on the CDK9 structure. Furthermore the side chains of Glu 92, Lys 20, and Lys 29 brings the phenyl of Phe 90 to a position deeper in the binding pocket, which also contributed to increase the contact area between flavopiridol and CDK9.

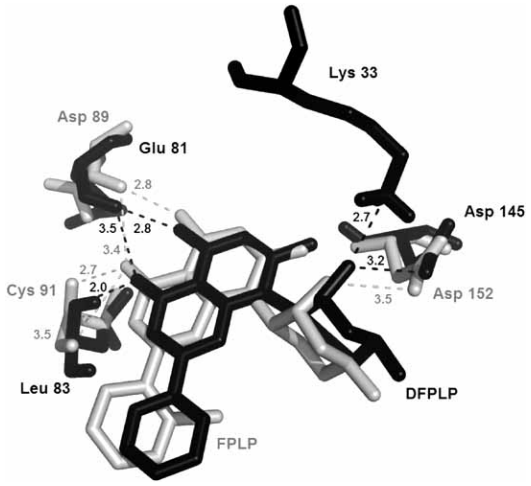

Fig. (7). Details of superposition of the complexes of deschloroflavopiridol (DFPLP) with CDK2 and flavopiridol (FPLP) with CDK9 showing intermolecular hydrogen bonds involving ligand and residues, indicated with dashed lines. The figure was generated with program Pymol [56]. CDK2 and DFPLP are presented as black stick and CDK9 and FPLP as light gray stick.

Most recently, a structural model for the binary complex of CDK9-CAN508 has been proposed using the same protocol described for the modeling of CDK9-flavopiridol [17]. This inhibitor, CAN508 (4-Arylazo-3,5-diaminopyrazole), proved to be a competitive inhibitor of CDK2-cyclin E with respect to ATP [17]. Cellular activity of CAN508 blocks proliferation of several tested cancer cell lines. Roscovitine a well-known CDK inhibitor, which has similar affinity for CDK9 [24] causes accumulation of p53 in cells treated at lower concentrations [17]. Analysis of the CDK selectivity

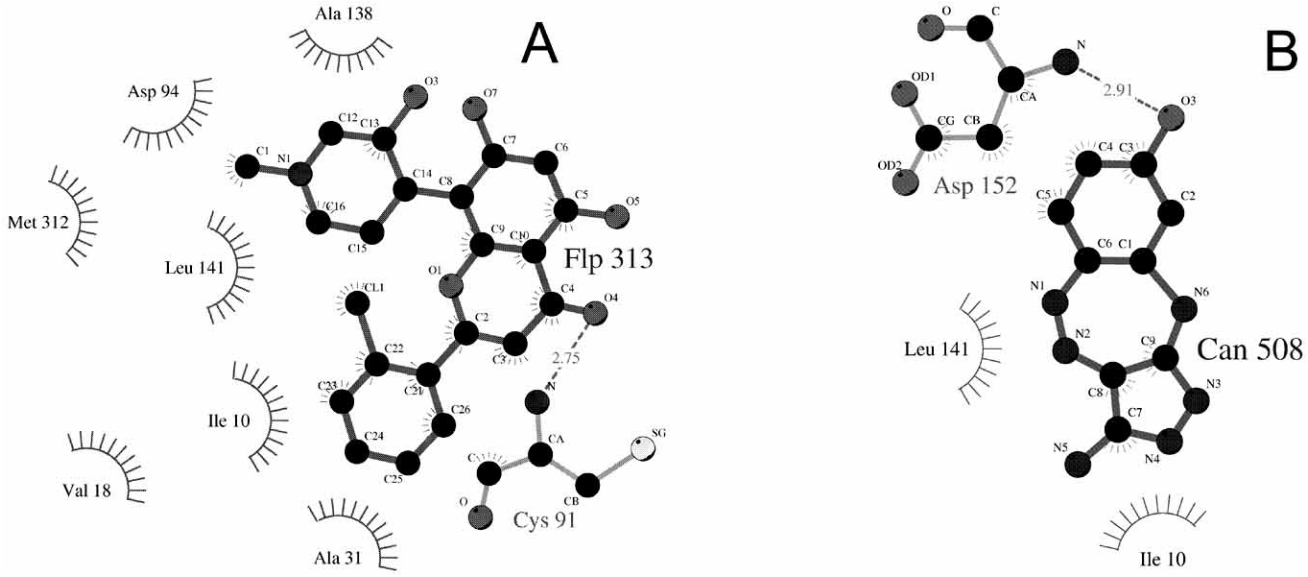

Fig. (6). Intermolecular hydrogen bonds for flavopiridol (A) and CAN508 (B) with ATP-binding pocket. Figure generated with Ligplot [57].

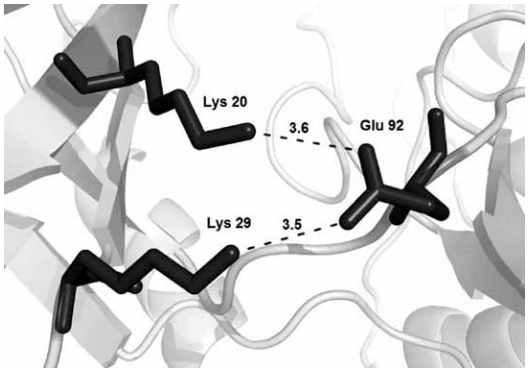

Fig. (8). Salt bridges, observed between Glu 92–Lys 20 and Glu 92–Lys 29 in the CDK9–flavopiridol. Figure generated with program Pymol [56], the CDK9 is presented as ribbon (light gray) and residues Lys 20, Lys 29 and Glu 92 are presented as stick (dark gray).

profiles indicates that inhibition of other CDKs (probably *via* combined effects on CDK2, CDK7, and CDK9) may be responsible for the antiproliferative and pro-apoptotic potency of CDK inhibitors [17]. However, the cellular activity of several 4-phenylazo-3,5-diamino-1*H*-pyrazole derivatives significantly exceeded that of olomoucine, thus, they represent good lead compounds for further structural optimization of specific CDK9 inhibitors [17], with applications in development of anticancer and anti-viral drugs.

The selectivity of CAN508 towards CDK9-cyclin T1 found during kinase assays prompted an investigation into the structural basis for this selectivity. Analysis of the modeled interactions between CAN508 and CDK9 (Fig. (**6**)) indicates the participation of Asp152 (which corresponds to Asp145 in CDK2) in an intermolecular hydrogen bond with the phenol- OH of the inhibitor. Intermolecular hydrogen-bond interactions corresponding to those with Glu81 and Leu83 observed in the CDK2-CAN508 [17] complex appear to be absent in the CDK9-CAN508 model. This was the first CDK inhibitor to show no participation of the molecular fork of CDK in intermolecular hydrogen bonds, previously described to be present in intermolecular hydrogen bonds in the structures of all CDK-inhibitor complexes studied so far [38]. In the CDK9 complex structure, CDK9 interactions with CAN508 are characterized by predominantly hydrophobic and van der Waals interactions between the protein and the 4-phenylazo moiety. Most of the intermolecular contacts between CDK9 and CAN508 involve a hydrophobic pocket formed by the residues Ile25, Val33, Phe103, Cys116, Leu156, Ala166, and Asp167. A structural comparison of both complexes (CDK2-CAN508 and CDK9-CAN508) indicates that the specificity of CAN508 for CDK9 does not stem from the establishment of intermolecular hydrogen bonds, because the CDK9-CAN508 complex presents a smaller number of hydrogen bonds when compared with CDK2-CAN508 complex. The most striking difference between the two complexes concerns the intermolecular contact area, which is significantly higher in the CDK9 complex (190 $Å^2$) than in the CDK2 complex (174 $Å^2$). Structural inspection of the interaction between CAN508 and CDK9 suggests that the inhibitor's specificity against CDK9 is probably due to the 4-phenylazo moiety, which affords a higher intermolecular contact area with CDK9 than that observed for the CDK2-CAN508 complex. Especially interesting is the presence of two salt bridges (Glu107-Lys35 and Glu107-Lys44) in the CDK9-CAN508 structure; these were also observed in the CDK9-flavopiridol complex and involve residues at interface between both lobes of the CDK9 structure, the overall result is an increase in the contact area between the CDK9 and CAN508. These salt bridges are not observed in the CDK2-CAN508 complex. A tighter ATP-binding pocket observed in the CDK9-CAN508 complex makes possible a higher number of intermolecular van der Waals contacts between CDK9 and CAN508.

The analysis of the charge distribution of the binding pockets indicates the presence of some charge complementarity between inhibitor and enzyme, nevertheless most of the binding pocket is hydrophobic in both structures. The overall analysis of the intermolecular interaction between CDK9 and inhibitors strongly indicates that we would expect higher intermolecular contact area and higher number of intermolecular hydrogen bonds for inhibitors with low IC50. This qualitative observation may help the guidance on exploring large chemical libraries, selecting potential new CDK inhibitor based on the intermolecular hydrogen bond pattern and contact area.

MOLECULAR FORK

It has been observed in several structures of CDK2 and CDK9 complexed with inhibitors the participation of a molecular fork, composed by a C=O group of Glu81 (Asp in CDK9) and the N-H and C=O group of Leu83 (Cys in CDK9), in intermolecular hydrogen bonds between CDK2 and CDK9 and the inhibitors. There are eighty structures of CDK2 complexed with inhibitors (search performed on the PDB [46] on January 2007). Analysis of the intermolecular hydrogen bond distances between CDK2 and all inhibitors that have atomic coordinates deposited in the PDB and also for the complexes of CDK2 with IPA, olomoucine, roscovitine, and flavopiridol strongly indicates the conservation of at least one member of the molecular fork in hydrogen bonding. This molecular fork, composed of two hydrogen bond acceptors (C=O) and one hydrogen bond donor (N-H), allows a wide range of different molecules to dock on to the ATP binding pocket, such as: olomoucine, isopentenyladenine, and roscovitine [47,48,39], staurosporine [49], purvalanols [50], indirubins [51], hymenialdisine [49], UCN-01[52], NU2058 [18], and diaminopyrazole derivatives [17]. All these inhibitors have pairs of hydrogen bond partners that show complementarity to the molecular fork on CDK2 and CDK9, most of them involving at least two hydrogen bonds with the molecular fork. The relative orientation of the inhibitor in the ATP-binding pockets of CDK2 and CDK9 locate one hydrogen bond donor close to C=O in Glu81 (Asp in CDK9) and/or Leu83 (Cys in CDK9), and an acceptor close to N-H in Leu83 (Cys in CDK9). Differences in the sequence of the molecular fork, observed between CDK2 and CDK9, is not expected to cause major differences in the intermolecular hydrogen bonds of the molecular fork, since it involves only main-chain atoms in the hydrogen bonds. Such simple paradigm is conserved in all CDK2-inhibitor complex structures solved so far. In all binary models obtained by

homology modeling for CDK9, this molecular fork is also conserved [40].

COMPLEX CDK9-CYCLIN

Human CDKs are inactive as monomers, and their activation needs binding to cyclins, a diverse family of proteins whose levels oscillate during the cell cycle, in the case of CDK9 the partner is (cyclin T or cyclin K). There is no structural information for cyclin T1, however recently the cyclin K structure has been solved by X-ray crystallography [53]. The structure of cyclin K opened the possibility of modeling of cyclin T1, since the sequence identity between them is over 42 %. This modeling allowed studies of the interaction of CDK9 and cyclin T1, using molecular modeling approaches. Two isoforms of CDK9 have been identified in the human genome cells, CDK9 (42kDa) and CDK9 (55kDa), which differ in their N-terminal domains. The association of these isoforms with cyclins K, T1, T2a, and T2b, results in the formation of eight structurally and functionally distinct P-TEFb. This binary complex shows that their CDK9-interacting surfaces present great structural differences, which could potentially be exploited for the design of cyclin-targeted inhibitors of the CDK9–cyclin K and CDK9–cyclin T1 complexes.

REFERENCES

[1] Hunt, T. *Curr. Opin. Cell Biol*., **1989**, *1*, 268.
[2] Fang, F.; Newport, J. W. *Cell*, **1991**, *66*, 731.
[3] Norbury, C.; Nurse, P. *Annu. Rev. Biochem*., **1992**, *61*, 441.
[4] Sherr, C. J. *Science*, **1996**, *274*, 1672.
[5] Morgan, D. O. *Annu. Rev. Cell Dev. Biol.*, **1997**,*13*, 261.
[6] Knockaert, M.; Greengard, P.; Meijer, L. *Trends Pharmacol. Sci.,* **2002**, *23*, 417.
[7] Loyer, P.; Trembley, J. H.; Katona, R.; Kidd, V. J.; Lahti, J. M. *Cell. Signalling,* **2005**, *17*, 1033.
[8] Schang, L. M. *Curr. Drug Targets: Infect. Disord.,* **2005**, *5*, 29.
[9] De Azevedo, W.F.Jr.; Mueller-Dieckmann, H.J.; Schulze-Gahmen, U.; Worland, P.J.; Sausville, E.; Kim S.-H. *Proc. Natl. Acad. Sci. USA*, **1996**, *93*, 2735.
[10] Dai, Y.; Grant, S. (2003) *Curr. Opin. Pharmacol.,* **2003**, *3*, 362.
[11] Sielecki, T. M.; Boylan, J. F.; Benfield, P. A.; Trainor, G. L. *J. Med. Chem.*, **2000**, *43*, 1.
[12] Fischer, P. M.; Lane, D. P. *Curr. Med. Chem*., **2000**, *7*, 1213.
[13] Richardson, H.E.; Stueland, C.S.; Thomas, J.; Russel, P.; Reed, S. I. *Genes Dev.*, **1990**, *4*, 1332.
[14] Peter, M. *Prog. Cell Cycle Res.*, **1997**, *3*, 99.
[15] Bourne, Y.; Watson, M. H.; Hickey, M. J.; Holmes, W.; Rocque, W.; Reed, S. I.; Tainer, J. A. *Cell*, **1996**, *84*, 863.
[16] Kim, S.-H.; Schulze-Gahmen, U.; Brandsen, J.; De Azevedo, W. F. Jr. *Prog. Cell Cycle Res*., **1996**, *2*, 137.
[17] Krystof, V.; Cankar, P.; Frysova, I.; Slouka, J.; Kontopidis, G.; Dzubak, P.; Hajduch, M.; Srovnal, J.; de Azevedo, W.F.Jr.; Orsag, M.; Paprskarova, M.; Rolcik, J.; Latr, A.; Fischer, P.M.; Strnad, M. *J. Med. Chem*., **2006**, *49*, 6500.
[18] Canduri, F. and De Azevedo, W. F. *Curr. Comput. Aided Drug Des.,* **2005**, *1,* 53.
[19] Malumbres, M.; Barbacid, M. *Natl. Rev. Can*., **2001**, *1*, 222.
[20] Soni, R.; O'Reilly, T.; Furet, P.; Muller, L.; Stephan, C.; Zumstein-Mecker, S.; Fretz, H.; Fabbro, D.; Chaudhuri, B. J. *Natl. Can. Inst.,* **2001**, *93*, 436.
[21] Damiens, E.; Baratte, B.; Marie, D.; Eisenbrand, G.; Meijer, L. *Oncogene*, **2001**, *20*, 3786.
[22] Edamatsu, H.; Gau, C.L.; Nemoto, T.; Guo, L.; Tamanoi, F. *Oncogene*, **2000**, *19*, 3059.
[23] Matushansky, I.; Radparvar, F.; Skoultchi, A.I. *Proc. Natl. Acad. Sci. USA,* **2000**, *97*, 14317.
[24] Benson, C.; Kaye, S.; Workman, P.; Garrett, M.; Walton, M.; de Bono, J. *Br. J. Cancer,* **2005***, 92*, 7.
[25] Chao, S.-H.; Fujinaga, K.; Marion, J.E.; Taube, R.; Sausville, E.A.; Senderowicz, A.M.; Peterlin, B.M.; Price, D.H. J. *Biol. Chem.,* **2005***, 275*, 28345.
[26] Agbottah, E.; de La Fuente, C.; Nekhai, S.; Barnett, A.; Gianella-Borradori, A.; Pumfery, A.; Kashanchi, F. *J. Biol. Chem.,* **2005***, 280*, 3029.
[27] Ortega, S.; Prieto, I.; Odajima, J.; Martin, A.; Dubus, P.; Sotillo, R.; Barbero, J.L.; Malumbres, M.; Barbacid, M. *Nat. Genet.,* **2003***, 35*, 25.
[28] Ljungman, M.; Paulsen, M.T. *Mol. Pharmacol.,* **2001***, 60*, 785.
[29] Chao, S.-H.; Price, D.H. *J. Biol. Chem.,* **2001**, *276*, 31793.
[30] Demidenko, Z.N.; Blagosklonny, M.V. *Cancer Res.*, **2004**, *64*, 3653.
[31] Whittaker, S.R.; Walton, M.I.; Garrett, M.D.; Workman, P. *Cancer Res.,* **2004**, *64*, 262.
[32] MacCallum, D.E.; Melville, J.; Frame, S.; Watt, K.; Anderson, S.; Gianella-Borradori, A.; Lane, D.P.; Green, S.R. *Cancer Res.,* **2005**, *65*, 5399.
[33] Lacrima, K.; Valentini, A.; Lambertini, C.; Taborelli, M.; Rinaldi, A.; Zucca, E.; Catapano, C.; Cavalli, F.; Gianella-Borradori, A.; MacCallum, D. E.; Bertoni, F. *Ann. Oncol.,* **2005**, *16*, 1169.
[34] Shan, B.; Zhuo, Y.; Chin, D.; Morris, C.A.; Morris, G.F.; Lasky, J.A. Cells. *J. Biol. Chem.,* **2005***, 280*, 1103.
[35] Havlicek, L.; Fuksova, K.; Krystof, V.; Orsag, M.; Vojtesek, B.; Strnad, M. *Bioorg. Med. Chem.,* **2005**, *13*, 5399.
[36] Moravcova, D.; Krystof, V.; Havlicek, L.; Moravec, J.; Lenobel, R.; Strnad, M. *Bioorg. Med. Chem. Lett.,* **2003***, 13*, 2989.
[37] Canduri, F.; Uchoa, H.B.; de Azevedo, W.F.Jr. *Biochem. Biophys. Res. Commun.,* **2004***, 324*, 661.
[38] De Azevedo, W.F.Jr.; Canduri, F.; Da Silveira, N.J.F. *Biochem. Biophys. Res. Commun,.* **2002***, 293*, 566.
[39] De Azevedo, W.F.Jr.; Gaspar, R.T.; Canduri, F.; Camera, J.C.Jr.; Silveira, N.J.F. *Biochem Biophys. Res. Commun.*, **2002**, *297*, 1154.
[40] Leopoldino A.M.; Canduri F.; Cabral H.; Junqueira M.; de Marqui A.B.T.; Apponi L.H.; da Fonseca I.O.; Domont G.B.; Santos D.S.; Valentini S.; Bonilla-Rodriguez G.O.; Fossey M.A.; de Azevedo Jr. W.F.; Tajara E.H.; *Protein Express. Purif.,* **2006**, *47*, 614.
[41] Sims, R.J.; Belotserkovskaya, III.R.; Reinberg, D. *Genes Dev.*, **2004**, *18*, 2437.
[42] Mortillaro, M.J.; Blencowe, B.J.; Wei, X.; Nakayasu, H,; Du, L.; Warren, S.L.; Sharp, P.A.; Berezney, R. *Proc. Natl. Acad. Sci. USA*, **1996**, *93*, 8253.
[43] De Falco, G.; Giordano, A. *Cancer Biol Ther*., **2002**, *1*, 342.
[44] Fu J, Yoon HG, Qin J, Wong J. *Mol. Cell Biol*., **2007**, *27*, 4641.
[45] Uchoa, H.B.; Jorge, G.E.; Freitas Da Silveira, N.J.; Camera, J.C. Jr.; Canduri, F.; De Azevedo, W.F.,Jr. *Biochem. Biophys. Res. Commun.,* **2004***, 325*, 1481.
[46] Berman, H.M.; Westbrook, J.; Feng, Z.; Gilliland, G.; Bhat, T.N.; Weissig, H.; Shindyalov, I.N.; Bourne, P.E. *Nucleic. Acids Res.*, **2002**, *28*, 235.
[47] Noble, M.E.; Endicott, J.A.; Johnson, L.N. *Science*, **2004**, *303*, 1800.
[48] Schultze-Gahmen, U.; Brandsen, J.; Jones, H.D.; Morgan, D.O.; Meijer, L.; Vesely, J. *Proteins*, **1995**, *22*, 378.
[49] Meijer, L.; Raymond, E. *Acc. Chem. Res.*, **2003**, *36*, 417.
[50] Losiewicz, M.D.; Carlson, B.A.; Kaur, G.; Sausville, E.A.; Worland, P.J. *Biochem. Biophys. Res. Commun.*, **1994**, *201*, 589.
[51] Kaur, G.; Stetler-Stevenson, M.; Sebers, S.; Worland, P.; Sedlacek, H.; Myers, C.; Czech, J.; Naik, T.; Sausville, E. *J. Natl. Can. Inst.*, **1992**, *84*, 1736
[52] Senderowicz, A.M.; Sausville, E.A. *J. Natl. Canc. Inst.*, **2000**, *92*, 376.
[53] Baek, K.B.; Brown, R.S.; Birrane, G.; Ladias, J.A. *J. Mol. Biol.,* **2007**, *366*, 563.
[54] Thompson, J.D.; Higgins, D.G.; Gibson T.J. *Nucleic Acids Res.*, **1994**, *22*, 4673.
[55] De Azevedo, W.F.Jr.; Canduri, F.; Silveira, N.J.F. *Biochem. Biophys. Res. Commun.,* **2002**, *293*, 566.
[56] DeLano, W.l. The PyMOL Molecular Graphics System. DeLano Scientific, San Carlos, CA, USA, **2002**. [http://www.pymol.org]
[57] Wallace, A.C.; Laskowski, R.A.; Thornton, J.M. *Prot. Eng.*, **1995**, *8*, 127.
[58] Tippmann H. F. *Brief Bioinform*., **2004**, *5*, 82.

Received: 06 November, 2007 Revised: 19 December, 2007 Accepted: 19 December, 2007